



Constitutive Model for HSC Confined by UHS and NS Transverse Reinforcements under Cyclic and Earthquake Loadings

M. Bastami

Assistant Professor, Department of Civil Engineering, University of Kurdistan, Sanandaj, Iran,
email: m.bastami@uok.ac.ir

ABSTRACT

In this paper, a cyclic constitutive model is developed for high-strength concrete (HSC) confined by ultra-high-strength and normal-strength transverse reinforcements (UHSTR and NSTR), with the intention of providing efficient modeling for the member and structural behavior of HSC in seismic regions. The model for HSC subjected to monotonic and cyclic loading, comprises four components; an envelope curve (for monotonic, cyclic and earthquake loadings), an unloading curve, a reloading curve, and a tensile unloading curve. It explicitly accounts for the effects of concrete compressive strength, the volumetric ratio of transverse reinforcement, yield strength of ties, tie spacing, and tie pattern. The proposed envelope curve models for confined HSC cover four options; namely, (1) rectangular (square) cross section with NSTR, (2) circular cross section with NSTR, (3) rectangular (square) cross section with UHSTR, and (4) circular cross section with UHSTR. Comparisons with test results showed that the proposed model provides a good fitting to a wide range of experimental results. The configuration of transverse reinforcement had a particularly large effect.

Keywords:

Constitutive model;
High-strength concrete;
Confined;
Ultra-high-strength
transverse reinforcement;
Normal-strength
transverse reinforcement;
Earthquake loading

1. Introduction

High-strength concrete (*HSC*) is normally used in high-rise buildings to reduce column sizes and increase available space, and in bridge structures to increase span lengths and cut down on the number of supporting piers or to make use of fewer beams on a given span length. High-strength concrete is also used to satisfy specific needs or special applications such as accelerated strength gain, durability, and modulus of elasticity [1]. Despite their adoption by the construction industry and their wide-spread application in non-seismic regions, their use in earthquake-prone areas has lagged behind, mainly due to concerns regarding the inelastic deformability of *HSC* columns under load reversals [2]. High-strength concrete is generally considered as a brittle material because failure during a compressive test occurs in a sudden and explosive manner. The issue of ductility is extremely important in structures subjected to

seismic loading conditions. In performing a structural analysis in such a region, the effect of earthquake loadings on the structure needs to be analyzed. Therefore, an understanding of material behavior of concrete and confining material (typically steel) subjected to cyclic loading is necessary in such analysis. There are experimental studies reported in literature for the behavior of unconfined normal strength concrete (*NSC*) subjected to cyclic axial compression [3-6]. Similar studies were reported for confined *NSC* (20-49MPa (2.9-7.1ksi)) subjected to cyclic axial compression [5, 7, 8, 9, 10]. Few experimental observations as such were reported for *HSC* in literature. The available deformational curves for unconfined and confined *NSC* represent the variation of axial stress with axial strain only. In the seismic design of reinforced concrete structures, a sufficient level of ductility is important for energy

absorption. With the increased use of *HSC* in structures, the issue of ductility improvements has become important. It is a common practice to use confining reinforcement in both earthquake resisting structures and other structures, to increase the ductility of the structural members. The computational analysis of reinforced concrete structures subjected to dynamic or cyclic loadings requires realistic stress-strain material models to reproduce the real behavior of the structure [11]. The utilization of experimental data in order to derive mathematical models to express physical behavior is imperative and widely used. On the other hand, the implementation of analytical methods for the purpose of optimizing the derived mathematical models is also necessary. Although valuable experimental verification is required to understand the member and structural behavior of high-strength materials (*HSM*) in seismic regions, the development of analytical modeling techniques can assist in this effort, particularly if they constitute part of a parametric analysis. Conducting a parametric analysis, though, especially when aiming at assessing complete high-rise buildings, is a very complicated issue due to uncertainties related to the mathematical representation of material properties [12].

2. Research Significance

In this paper, a constitutive model for description of the response of *HSC* confined by *UHSTR* and *NSTR* for square and circular cross sections under general cyclic loading is presented. Compared to previous ones, the model presents several advantages. It allows considering all the hysteretic characteristics of the complex behavior of concrete in a simple and practical way. It can also be used to simulate the cyclic response of *HSC* subjected to general load conditions, including unloading or reloading or mixed hysteretic loops involving the transition from compression to tension stresses or vice versa. Moreover, all the required input data can be obtained through conventional laboratory monotonic and cyclic compression tests. This is an important issue which determines the applicability of the present model in engineering practice. The model has been validated by comparison with available experimental results provided by different authors.

3. Existing Constitutive Models

Investigations on stress-strain curves for concrete subjected to cyclic loading dates back to the early 1960s. Several definitions are reported in literature for the unloading and reloading branches of the stress-strain curves for unconfined as well as confined *NSC*. Sinha et al [3] suggested a second degree parabola for the unloading curve and a straight line for the reloading curve. It was based on experimental observations for unconfined concrete. Karsan and Jirsa [4] proposed second degree parabolas for unloading and reloading branches for unconfined concrete. It was based on the plastic strain ratio. A more simplified concrete model is proposed by Blakely and Park [13], in this model unloading and reloading is assumed to take place along a line without energy dissipation or stiffness deterioration for strains smaller or equal to the strain corresponding to peak stress. Mander et al [14] proposed a reversal stress-strain curve from the compressive loading curve as the unloading curve and reloading path composed of a linear relationship and a parabolic transition curve. This analytical work was supported by the experimental work reported [8] for spirally reinforced circular columns and for columns with rectangular cross sections. The Otter and Naaman [15] model was originally developed for plain and fiber-reinforced concrete, but can also be applied to confined concrete with little modification. The model uses the unloading strain, the plastic strain and the reloading point as end points of the unloading and reloading curves. The unloading curve is described by a polynomial equation were derived by fitting experimental results. A simpler equation is proposed for the reloading branch consisting one linear expression. Chang and Mander [16] proposed an advanced model to simulate the hysteretic behavior of confined and unconfined concrete in both cyclic compression and tension for both ordinary as well as high-strength concrete including, the first time, effects of degradation produced by partial looping and a crack-closing model. The equation used by the authors for the unloading and reloading curves was a general Ramberg and Osgood [17] equation adjusted by a series of parameters: the slope at the origin and the slope at the end of each curve. Martinez-Rueda and Elnashai [18] modified the model by Mander et al [14] based on the observed

lack of numerical stability of Mander's model, particularly under large displacements. Among the modifications made was to include the effect of degradation in stiffness and strength due to cyclic loading and the introduction of three different definitions of plastic strain corresponding to low, intermediate, and high-strain ranges and accounting for the softening of concrete with progression of strains. Lokuge et al [19] developed a constitutive model for high-strength concrete with uniform lateral confinement subjected to cyclic axial compression. It is based on the testing program carried out for normal and high strength concrete. The envelope curve of the proposed model is based on the 24 experimental results reported by Candappa et al [20] as well as previous work presented by Attard and Setunge [21]. Unloading and reloading branches were developed based on the 24 tests carried out by the authors. The parabolic transition curve is the one proposed by Mander et al [8], and plastic strain is a modified version of that proposed by Mander et al [8]. Konstantinidis et al [12] proposed a constitutive model for describing the hysteretic stress-strain behavior of *HSC* under reversed cyclic loading. The envelope curve is derived from the results of uniaxial, monotonic, compression loading tests of 108 large-scale specimens. It explicitly accounts for the effects of concrete compressive strength, the volumetric ratio of transverse reinforcement, yield strength of ties, tie spacing, and tie pattern. The proposed model is implemented in the finite element program *ADAPTIC*, with a view to analyzing *HSC* members under reversed cyclic loading. Sima et al [11] developed a constitutive model for *NSC* subjected to cyclic loadings in both compression and tension. Particular emphasis has been paid to the description of the strength and stiffness degradation produced by the load cycling in tension and compression, the shape of unloading and reloading curves and the transition between opening and closing of cracks. Two independent damage parameters in compression and in tension have been introduced to model the concrete degradation due to increasing loads. Lavassani et al [22] developed a hysterical constitutive law for reinforced concrete subjected to earthquake loadings in both compression and tension that was selected for refinement on modeling the hysteretic behavior of concrete structures under earthquake loadings by finite element codes. The fundamental framework of the presented concept is

the stress-based elastoplastic-damage-fracture (*EPFD*) theory. The relationships used in the compression domain include the elasto-plastic fracture behavior. The main novelty of the proposed hysterical constitutive law for reinforced concrete lies in the fact that the foundation of constitutive formulations are based on thermodynamics framework and all the required parameters can be obtained through simple formal tests.

4. Proposed Model for Confined HSC

4.1. Envelope Curve

It is commonly accepted by most researchers [4, 6, 23], among others, that the envelope curve for a concrete subjected to cyclic axial compression can be approximated by the monotonic stress-strain curve of concrete. A similar conclusion was also drawn for *HSC* columns confined with high-yield steel (*HYS*) tested by Li et al [24]. A three-branch stress-strain curve proposed to model the response of high-strength rectangular and circular concrete confined by *NSTR* that is based on Kappos and Konstantinidis [25] model and conducting regression analyses on the existing experimental data as Eqs. (1-13):

Ascending Branch:

$$\sigma_c = f'_{cc} \left[\frac{\lambda(\varepsilon_c / \varepsilon_{cc})}{\lambda - 1 + (\varepsilon_c / \varepsilon_{cc})^\lambda} \right] \quad 0 < \varepsilon_c \leq \varepsilon_{cc} \quad (1)$$

$$\lambda = \frac{E_c}{E_c - E_{sec}}; \quad E_{sec} = f'_{cc} / \varepsilon_{cc}; \quad (2)$$

$$E_c = 3320 \sqrt{f'_c} + 6900; \quad \varepsilon_{co} = \left(\frac{f'_c}{E_c} \right) \left(\frac{r}{r-1} \right) \\ r = \frac{f'_c}{17} + 0.8 \quad (3)$$

Descending Branch:

$$\sigma_c = f'_{cc} \left[1 - \frac{\eta(\varepsilon_c - \varepsilon_{cc})}{\varepsilon_{0.5f'_c} - \varepsilon_{cc}} \right] \geq 0.3 f'_{cc} \quad \varepsilon_c > \varepsilon_{cc} \quad (4)$$

For rectangular (square) confined section: $h = 0.5$

$$\alpha = \left(1 - \frac{\sum_{i=1}^n C_i^2}{6b_c d_c} \right) \left(1 - \frac{s}{2b_c} \right) \left(1 - \frac{s}{2d_c} \right) \quad (5)$$

$$f'_{cc} = 0.85 f'_c + 10.3 (\alpha \rho_h f_{yh})^{0.4};$$

$$\varepsilon_{cc} = \varepsilon_{co} \left[1 + 32.8 \left(\frac{\alpha \rho_h f_{yh}}{f'_c} \right)^{1.9} \right]$$

$$\varepsilon_{0.5 f'_{cc}} = \varepsilon_{co} + 0.091 \left(\frac{\alpha \rho_h f_{yh}}{f'_c} \right)^{0.8}$$

For circular confined section: h=0.14

$$\text{Circular hoops: } \alpha = \left(1 - \frac{s}{2d_s} \right)^2;$$

$$\text{Circular spirals: } \alpha = \left(1 - \frac{s}{2d_s} \right)$$

$$f'_{cc} = 0.85 f'_c + 19 (\alpha \rho_h f_{yh})^{0.4}$$

$$\varepsilon_{cc} = \varepsilon_{co} \left[1 + 32.8 \left(\frac{\alpha \rho_h f_{yh}}{f'_c} \right)^{1.03} \right];$$

$$\varepsilon_{0.5 f'_{cc}} = \varepsilon_{co} + 0.091 \left(\frac{\alpha \rho_h f_{yh}}{f'_c} \right)^{0.8}$$

Also, a three-branch stress-strain curve proposed to model the response of high-strength rectangular and circular concrete confined by UHSTR that is based on Li et al [26-27] model and conducting regression analyses on the existing experimental data as Eqs. (14-23):

Ascending Branch:

$$\sigma_c = f'_{cc} \left[\frac{\lambda (\varepsilon_c / \varepsilon_{cc})}{\lambda - 1 + (\varepsilon_c / \varepsilon_{cc})^\lambda} \right] \quad 0 < \varepsilon_c \leq \varepsilon_{cc} \quad (14)$$

$$\lambda = \frac{E_c}{E_c - E_{sec}}; \quad E_{sec} = f'_{cc} / \varepsilon_{cc}; \quad (15)$$

$$E_c = 3320 \sqrt{f'_c} + 6900; \quad \varepsilon_{co} = \left(\frac{f'_c}{E_c} \right) \left(\frac{r}{r-1} \right) \quad (16)$$

$$r = \frac{f'_c}{17} + 0.8$$

Descending Branch:

$$\sigma_c = f'_{cc} - \gamma \left(\frac{f'_{cc}}{\varepsilon_{cc}} (\varepsilon_c - \varepsilon_{cc}) \right) \geq 0.4 f'_{cc} \quad \varepsilon_c > \varepsilon_{cc} \quad (17)$$

(6) **For rectangular (square) confined section:**

$$(7) \quad \gamma = \begin{cases} (0.048 f'_c - 2.14) - (0.098 f'_c - 4.57) \times \\ 0.07 \\ 0.10 \end{cases}$$

$$(8) \quad \begin{cases} \left(\frac{0.5 \alpha \rho_h f_{yh}}{1 - \rho_g} \right)^{\frac{1}{3}} & f'_c > 75 \text{ MPa}, f_{yh} \leq 550 \text{ MPa} \\ f'_c \leq 80 \text{ MPa}, f_{yh} > 1200 \text{ MPa} \\ f'_c > 80 \text{ MPa}, f_{yh} > 1200 \text{ MPa} \end{cases} \quad (18)$$

$$(10)$$

$$f'_{cc} = f'_c \left[-1.254 + 2.254 \times \right.$$

$$(11)$$

$$\left. \sqrt{1 + 24.614 \left(\frac{0.5 \alpha \rho_h f_{yh}}{1 - \rho_g} \right)^2} - \right. \\ \left. 6.2 \left(\frac{0.5 \alpha \rho_h f_{yh}}{1 - \rho_g} \right)^2 \right] \quad (19)$$

$$(12) \quad \varepsilon_{cc} = \begin{cases} \varepsilon_{co} \left[2.0 + (87 - 1.06 f'_c) \left(\frac{0.5 \alpha \rho_h f_{yh}}{f'_c (1 - \rho_g)} \right)^{0.5} \right] \\ \varepsilon_{co} \left[2.0 + (53.4 - 0.42 f'_c) \left(\frac{0.5 \alpha \rho_h f_{yh}}{f'_c (1 - \rho_g)} \right)^{0.5} \right] \end{cases}$$

$$(13) \quad \begin{cases} f'_c \leq 50 \text{ MPa} \\ f'_c > 50 \text{ MPa} \end{cases} \quad (20)$$

For circular confined section:

$$(14) \quad \gamma = \begin{cases} 0.2 & f'_c \leq 80 \text{ MPa}, f_{yh} \leq 550 \text{ MPa} \\ 0.08 & f'_c \leq 80 \text{ MPa}, f_{yh} > 1200 \text{ MPa} \\ 0.2 & f'_c > 80 \text{ MPa}, f_{yh} > 1200 \text{ MPa} \end{cases} \quad (21)$$

$$f'_{cc} = f'_c \left[-0.413 + 1.413 \right]$$

$$(15) \quad \left. \sqrt{1 + 11.74 \left(\frac{0.5 \alpha \rho_h f_{yh}}{1 - \rho_g} \right) - 2 \left(\frac{0.5 \alpha \rho_h f_{yh}}{1 - \rho_g} \right)} \right] \quad (22)$$

$$\varepsilon_{cc} = \begin{cases} \varepsilon_{co} \left[1.0 + (120 - 1.554 f'_c) \left(\frac{0.5 \alpha \rho_h f_{yh}}{f'_c (1 - \rho_g)} \right)^{0.5} \right] \\ \varepsilon_{co} \left[1.0 + (71.4 - 0.623 f'_c) \left(\frac{0.5 \alpha \rho_h f_{yh}}{f'_c (1 - \rho_g)} \right)^{0.5} \right] \end{cases} \quad (23)$$

$f'_c \leq 50 MPa$

$f'_c > 50 MPa$

4.2. Unloading and Reloading Curves

As it has been observed by many researchers [3, 4, 6], when a concrete specimen is monotonically loaded up to a certain strain level and then unloaded to a zero stress level in a typical cyclic test, the unloading curve is concaved from the unloading point and characterized by high stiffness at the beginning [11]. The stiffness gradually decreases and becomes very flat at low stress levels and the residual plastic strains are considerably reduced. When reloading is performed from zero stress up to the envelope curve, it has been observed that the curve is rather flat in almost all of its length. Herein, a power type equation is proposed by conducting regression analyses on the existing experimental data for the unloading curve of concrete, and a linear type equation is used for the reloading curve as Eqs. (24) to (31).

Unloading Curve:

$$\sigma_c = \left(\frac{1 - \left(\frac{\varepsilon_c - \varepsilon_{un}}{\varepsilon_{pl} - \varepsilon_{un}} \right)}{1 + 1.3 \left(\frac{\varepsilon_c - \varepsilon_{un}}{\varepsilon_{pl} - \varepsilon_{un}} \right)} \right)^{1.3} \sigma_{un} \quad (24)$$

$$\varepsilon_{pl} = \varepsilon_{un} - \frac{\sigma_{un}}{E_r} \quad 0 \leq \varepsilon_{un} \leq \varepsilon_{0.35 f'_{cc}} \quad (25)$$

$$E_r = E_c \left[\frac{(\sigma_{un} / E_c \varepsilon_{cc}) + 0.6}{(\varepsilon_{un} / \varepsilon_{cc}) + 0.6} \right] \quad (26)$$

$$\varepsilon_{pl} = \varepsilon_{un} - \frac{\sigma_{un} (\varepsilon_{un} + a \sqrt{\varepsilon_{un} \varepsilon_{cc}})}{\sigma_{un} + E_c a \sqrt{\varepsilon_{un} \varepsilon_{cc}}} \quad \varepsilon_{un} > \varepsilon_{0.35 f'_{cc}} \quad (27)$$

$$a = \max \left\{ \frac{\varepsilon_{cc}}{\varepsilon_{cc} + \varepsilon_{un}}, \frac{0.09 \varepsilon_{un}}{\varepsilon_{cc}} \right\} \quad (28)$$

The relationship proposed for plastic strain has good results. The equation proposed for the unloading branch includes the mean features of the unloading curves obtained experimentally, such as the curvature of the curve, the initial stiffness, the final stiffness and the strain-plastic strain ratio.

Reloading Curve:

$$\sigma_c = \sigma_{ro} + E_{c1} (\varepsilon_c - \varepsilon_{ro}) \quad (29)$$

$$E_{c1} = \frac{\sigma_{ro} - \sigma_{new}}{\varepsilon_{ro} - \varepsilon_{un}} \quad (30)$$

$$\sigma_{new} = \sigma_{un} (1 - 0.09 \sqrt{\varepsilon_{un} / \varepsilon_{co}}) + 0.08 \sigma_{ro} \quad (31)$$

The reloading response is modeled by a linear curve as is done by most researchers [8, 10, 18, 28], among others.

Tensile unloading branches:

The tension strength is given by following equations, when unloading from a compressive branch:

$$\sigma_t = f'_t (1 - \varepsilon_{pl} / \varepsilon_{cc}) \quad (32)$$

$$\sigma_t = \begin{cases} 0 & \varepsilon_{pl} > \varepsilon_{cc} \\ E_t (\varepsilon_c - \varepsilon_{pl}) & \varepsilon_{pl} < \varepsilon_{cc} \end{cases} \quad (33)$$

$$E_t = \sigma_t / \varepsilon_t \quad (34)$$

$$\varepsilon_t = f'_t / E_t \quad (35)$$

When $\varepsilon_c > (\varepsilon_t - \varepsilon_{pl})$, cracks open and tensile strength of concrete for all subsequent loadings is assumed to be zero.

5. Model Verification- Comparison with Test Results

5.1. Envelope Curve Model Verification

The envelope curve model has been verified by comparing proposed model with experimental results [26, 29, 30, 31] those from selected column tests presented in Tables (1) to (4) including detailed specification of them. The comparisons included square, rectangular and circular columns with a wide range of confinement parameters and concrete strengths. Sample comparisons selected from different research programs, shown in Figures (1) to (4), indicate a good agreement between the proposed model and the experimental results.

Figure (1) is the comparison between stress-strain

Table 1. HSC specimens properties for square test unites with NSTR.

No.	Ref.	Unit No.	f'_c (MPa)	Section (mm)	No. of Bars	f_{yg} (MPa)	ρ_g (%)	S (mm)	f_{yh} (MPa)	ρ_h (%)
1	Nagashima et al [29]	HL06LA	118	225×225	12	378	2.4	45	807	2.03
2	Nagashima et al [29]	HL08LA	118	225×225	12	378	2.4	35	807	2.61
3	Cusson and Paultre [30]	5A	99.9	235×235	4	420	3.6	50	705	2.9
4	Cusson and Paultre [30]	5B	99.9	235×235	8	450, 406	3.6	50	770	3.43
5	Cusson and Paultre [30]	5C	99.9	235×235	12	450, 406	3.6	50	770	3.62
6	Cusson and Paultre [30]	5D	99.9	235×235	12	450, 406	3.6	50	770	4.69
7	Li et al [26]	1A	60	240×240	4	443	0.8	20	445	2.63
8	Li et al [26]	2A	60	240×240	8	443	1.6	20	445	4.48
9	Li et al [26]	4A	60	240×240	4	443	0.8	35	445	1.5
10	Li et al [26]	1B	72.3	240×240	4	443	0.8	20	445	2.63
11	Li et al [26]	5B	72.3	240×240	8	443	1.6	35	445	2.56

Table 2. HSC specimens properties for circular test unites with NSTR.

No.	Ref.	Unit No.	f'_c (MPa)	Section (mm)	No. of Bars	f_{yg} (MPa)	d_b (%)	S (mm)	f_{yh} (MPa)	ρ_h (%)
1	Li et al [26]	3A	63	240-Circular	6	443	6	20	445	1.53
2	Li et al [26]	6A	63	240-Circular	6	443	6	35.5	445	0.82
3	Li et al [26]	3B	72.3	240-Circular	6	443	6	20	445	1.53
4	Li et al [26]	6B	72.3	240-Circular	6	443	6	35.5	445	0.82
5	Razvi and Saatcioglu [31]	CC-8	105.4	225-Circular	8	660	6.3	70	660	1.2
6	Razvi and Saatcioglu [31]	CC-10	105.4	225-Circular	8	400	11.3	60	400	3.67
7	Razvi and Saatcioglu [31]	CC-11	105.4	225-Circular	8	660	6.3	60	660	1.2

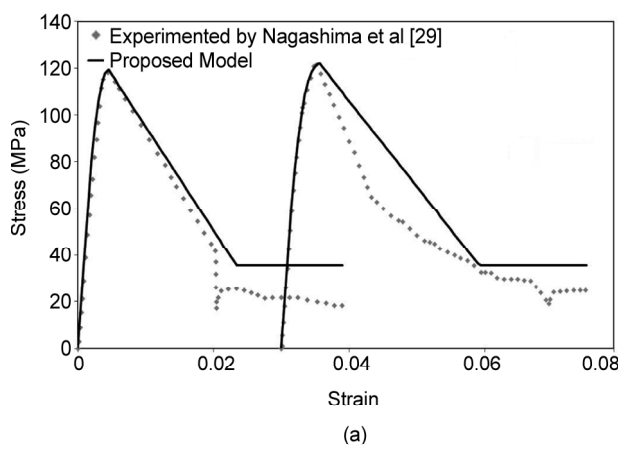
Table 3. HSC specimens properties for square test unites with UHSTR.

No.	Ref.	Unit No.	f'_c (MPa)	Section (mm)	No. of Bars	f_{yg} (MPa)	ρ_g (%)	S (mm)	f_{yh} (MPa)	ρ_h (%)
1	Nagashima et al [29]	LH08LA	57.3	225×225	12	378	1.86	55	1386	1.66
2	Nagashima et al [29]	HH15LA	58.5	225×225	12	378	1.86	45	1366	3.9
3	Li et al [26]	1HB	52	240×240	8	443	1.6	20	1318	5
4	Li et al [26]	3HB1	52	240×240	8	443	1.6	35	1318	2.86
5	Li et al [26]	3HC1	82.5	240×240	8	443	1.6	35	1318	2.86

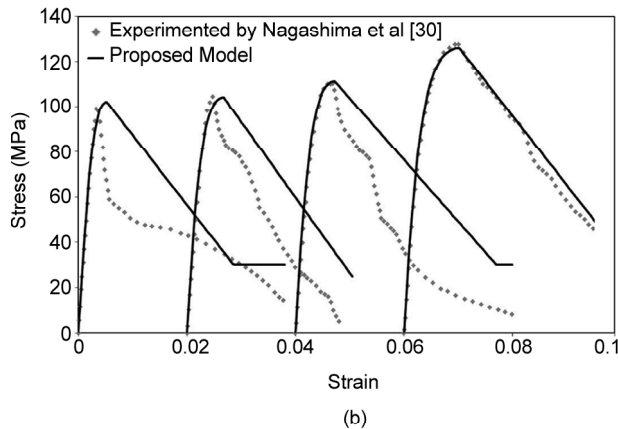
Table 4. HSC specimens properties for circular test unites with UHSTR.

No.	Ref.	Unit No.	f'_c (MPa)	Section (mm)	No. of Bars	f_{yg} (MPa)	d_b (%)	S (mm)	f_{yh} (MPa)	ρ_h (%)
1	Li et al [26]	2HB	52	240-Circular	6	443	6.4	20	1318	2.94
2	Li et al [26]	4HC	82.5	240-Circular	6	443	6.4	35	1318	1.67
3	Razvi and Saatcioglu [31]	CC-14	78.2	225-Circular	8	851	7.5	60	1000	1.59
4	Razvi and Saatcioglu [31]	CC-16	78.2	225-Circular	8	796	7.5	60	1000	1.59

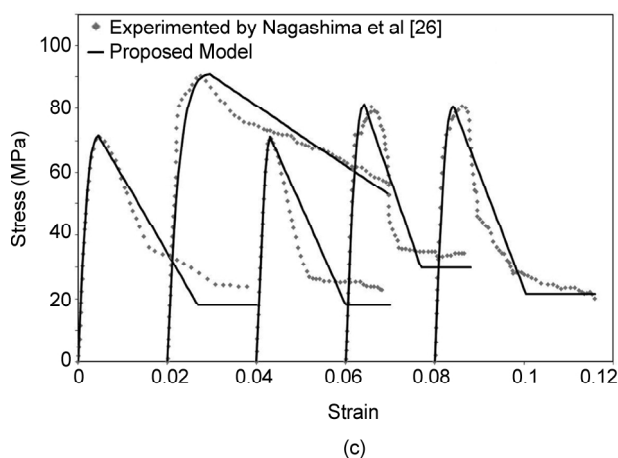
curves under monotonic compression loading of the HSC specimens for square test unites with *NSTR*, see Table (1) and [26, 29, 30], and that of the proposed model. The stress-strain curve of the proposed model fits the experimental results well especially in ascending branch and maximum point although for Nagashima et al [29] and Cusson and Paultre [30] data. Figure (2) is the comparison between stress-strain curves under monotonic compression loading of the HSC specimens for circular test specimens with *NSTR*, see Table (2) and



(a)

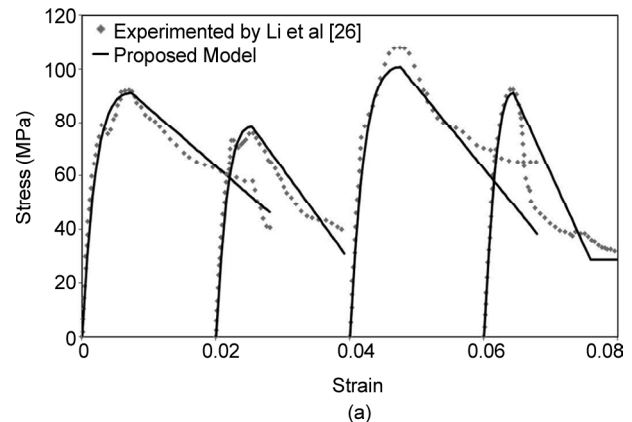


(b)

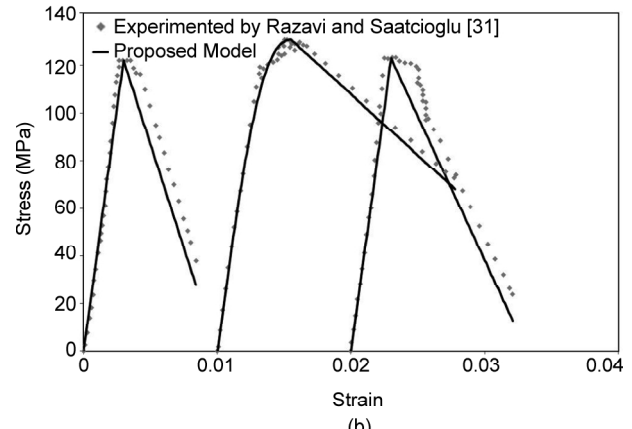


(c)

Figure 1. Comparison of experimental data with proposed model for square cross section confined by *NSTR*.

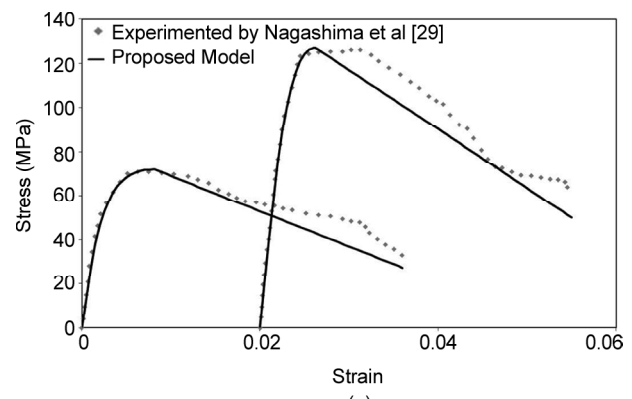


(a)

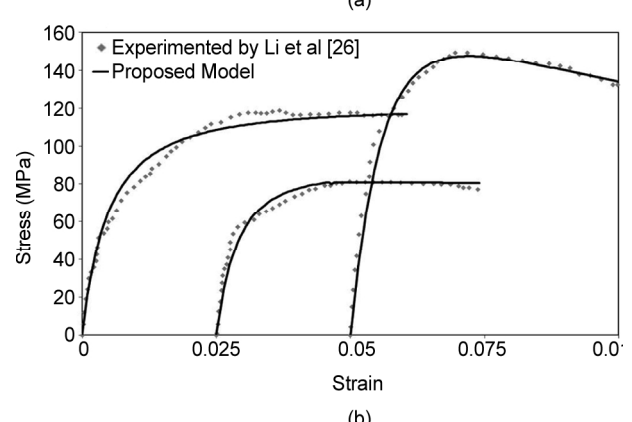


(b)

Figure 2. Comparison of experimental data with proposed model for circular cross section confined by *NSTR*.



(a)



(b)

Figure 3. Comparison of experimental data with proposed model for square cross section confined by *UHSTR*.

[26, 31], and that of the proposed model. The proposed model in this study agrees quite well with the experimental results. Figure (3) is the comparison between stress-strain curves under monotonic compression loading of the HSC specimens for square test specimens with *UHSTR*, see Table (3) and [26, 31], and that of the proposed model. The proposed model agrees with the test results fairly well especially with those of Li et al [26] while at the same time it underestimates the test results of Nagashima et al [29]. Figure (4) is the comparison between stress-strain curves under monotonic compression loading of the HSC specimens for circular test unites with *UHSTR*, see Table (4) and Li et al

[26, 31], and that of the proposed model. The proposed model is in good agreement with the test results.

5.2. Cyclic Constitutive Model Verification for Confined HSC

In the case of cyclic compression, results from works performed by Muguruna et al [32] and Li et al [26] have been considered as Table (5). Figures (5) to (8) present the experimental result [26, 32] and analytical predictions of the proposed model. As shown in Figures (5) to (8), it was found the assumption that the monotonic loading curve represents the skeleton curve of the stress-strain curves under cyclic loading is still valid, regardless of the concrete compressive strength and the yield strength of transverse reinforcement. Also, in general, the proposed model is in good agreement with the test results. Better agreement is achieved with the results of Li et al [26] than with those of Muguruna et al [32] with both test data sets being overestimated by the model. Further experimental results for circular cross section with *NSTR* and *UHSTR* are needed in order to establish well-founded models and to improve the proposed constitutive model.

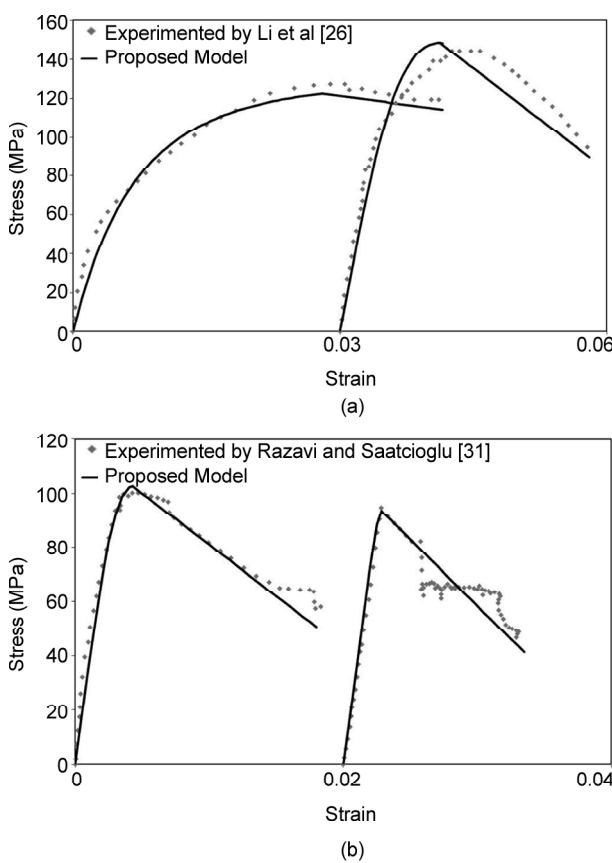


Figure 4. Comparison of experimental data with proposed model for circular cross section confined by UHSTR.

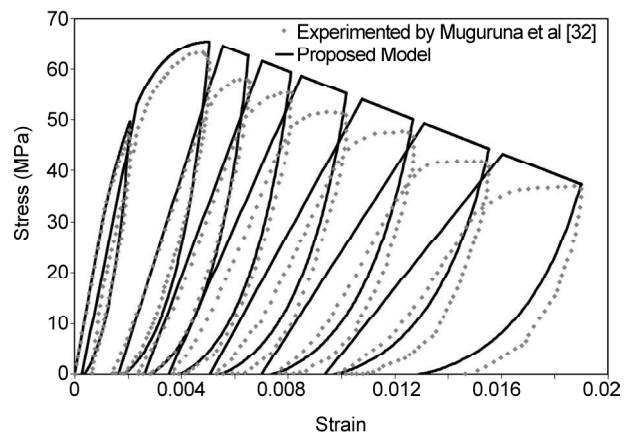


Figure 5. Comparison of experimental data for Specimen PS5-7R tested by Muguruna et al [32] and proposed cyclic constitutive model.

Table 5. HSC specimens properties for square test unites with UHSTR for cyclic compression loading.

No.	Ref.	Unit No.	f'_c (MPa)	Section (mm)	No. of Bars	S (mm)	f_{yh} (MPa)	ρ_h (%)
1	Muguruna et al [32]	PS5-7R	56.8	147.4×147.4	0	50	1360	4.26
2	Muguruna et al [32]	PD5-9R	80.4	147.4×147.4	0	50	1360	4.26
3	Li et al [26]	3HB3	52	240×240	8	35	1318	2.86
4	Li et al [26]	3HC3	82.5	240×240	8	35	1318	2.86

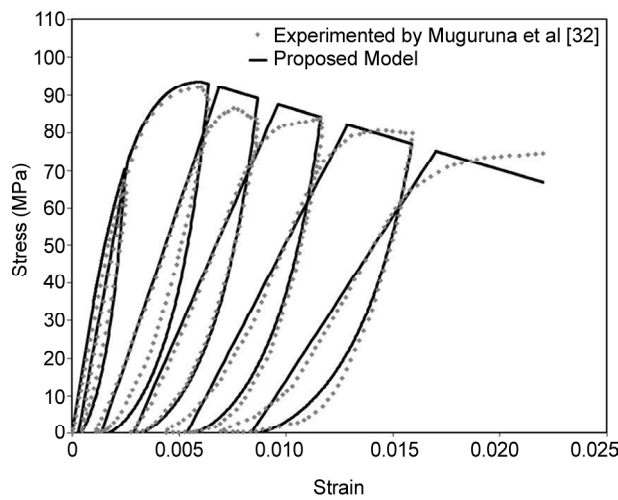


Figure 6. Comparison of experimental data for Specimen PD5-9R tested by Muguruna et al [32] and proposed cyclic constitutive model.

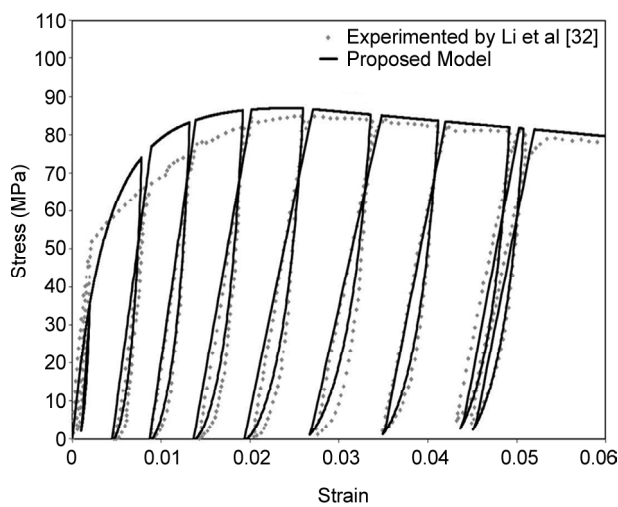


Figure 7. Comparison of experimental data for Specimen 3HB3 tested by Li et al [26] and proposed cyclic constitutive model.

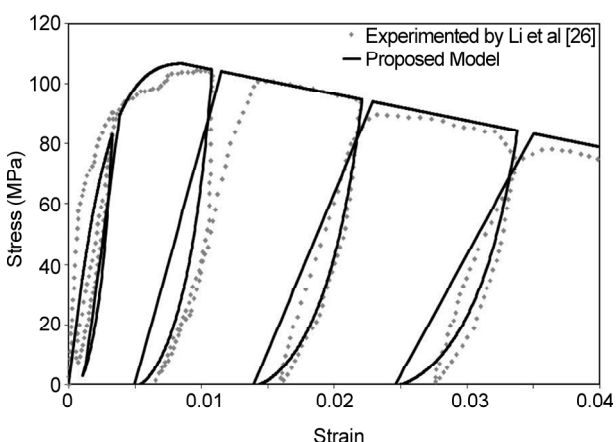


Figure 8. Comparison of experimental data for Specimen 3HC3 tested by Li et al [26] and proposed cyclic constitutive model.

6. Conclusions

In this work, a cyclic constitutive model is developed for HSC confined by normal-strength and ultra-high-strength transverse reinforcement leads to the following conclusions:

- ✓ The proposed envelope curve models for confined HSC cover four options; namely, (1) rectangular (square) cross section with *NSTR*, (2) circular cross section with *NSTR*, (3) rectangular (square) cross section with *UHSTR*, and (4) circular cross section with *UHSTR*.
- ✓ The proposed compression unloading, reloading curves and plastic strain are in good agreement with the experimental results.
- ✓ The proposed monotonic loading curve forms an envelope of curves for the cyclic loading.
- ✓ The most significant parameter affecting the shape of the stress-strain curve of confined concrete for all section shapes was the quantity of confining reinforcement, in the form of spirals for circular columns, or rectangular hoops or cross ties for square or rectangular columns.
- ✓ The configuration of transverse reinforcement had a particularly large effect.
- ✓ The proposed model provides good agreement with the test results, and this model would be sufficiently accurate for application in nonlinear response analyses although there is a little discrepancy with the test results.
- ✓ The relationship proposed for plastic strain yields good results. The equation proposed for the unloading branch includes the mean features of the unloading curves obtained experimentally, such as the curvature of the unloading curve, the initial unloading stiffness, the final unloading stiffness and the unloading strain-plastic strain ratio.

References

1. Ralls, M.-L. and Carrasquillo, R. (1994). "Texas High-Strength Concrete Bridge Project", Public Roads, **57**(4), 1-7.
2. ACI Committee 441 (1997). "State of the Art Report on High Strength Concrete", *ACI Structural Journal*, **94**(3), 323-335.
3. Sinha, B.P., Gerstle, K.H., and Tulin, L.G. (1964). "Stress-Strain Relations for Concrete under

- Cyclic Loading”, *ACI Structural Journal*, **61**(2), 195-211.
4. Karsan, I.D. and Jirsa, J.O. (1969). “Behavior of Concrete under Compressive Loadings”, *Journal of Structural Engineering, ASCE*, **95**(ST12), 2543-2563.
 5. Desayi, P., Iyengar, K.T.S.R., and Reddy, T.S. (1979). “Stress-Strain Characteristics of Concrete Confined in Steel Spirals under Repeated Loading”, *Material and Structures*, **12**(71), 375-383.
 6. Bahn, B.Y. and Hsu, T.T.C. (1998). “Stress-Strain Behavior of Concrete under Cyclic Loading”, *ACI Material Journal*, **95**(2), 178-193.
 7. Shah, S.P., Fafitis, A., and Arnold, R. (1983). “Cyclic Loading of Spirally Reinforced Concrete”, *Journal of Structural Engineering, ASCE*, **109**(7), 1695-1710.
 8. Mander, J.B., Priestley, J.N., and Park, R. (1988a). Observed Stress-Strain Behavior on Confined Concrete”, *Journal of Structural Engineering, ASCE*, **114**(8), 1827-1849.
 9. Watanabe, F. and Muguruma, H. (1988). “Toward the Ductility Design of Concrete Members-Overview of Researchers in Kyoto University”, *Proceedings of the Pacific Concrete Conference*, 89-100.
 10. Sakai, J. and Kawashima, K. (2000). “An Unloading and Reloading Stress-Strain Model for Concrete Confined by Tie Reinforcements”, *Proceedings of the 12th World Conference on Earthquake Engineering (12WCEE 2000)*, Auckland, New Zealand, The New Zealand Society for Earthquake Engineering, Wellington, New Zealand, 1-8.
 11. Sima, J.F., Roca, P., and Molins, C. (2008). “Cyclic Constitutive Model for Concrete”, *Journal Engineering Structures*, **30**, 695-706.
 12. Konstantinidis, K.K., Kappos, A.J., and Izzuddin, B.A. (2007). “Analytical Stress-Strain Model for High-Strength Concrete Members under Cyclic Loading”, *Journal of Structural Engineering, ASCE*, **133**(4), 484-494.
 13. Blakely, R.W.G and Park R. (1973). “Prestressed Concrete Sections with Cyclic Flexure”, *Journal of the Structural Divison, ASCE*, **98**(ST8), 1717-1742.
 14. Mander, J.B., Priestley, M.J.N., and Park, R. (1988b). “Theoretical Stress-Strain Model for Confined Concrete”, *Journal of Structural Engineering, ASCE*, **114**(8), 1804-1826.
 15. Otter, D.E. and Naaman, A.E. (1989). “Model for Response of Concrete to Random Compressive Loads”, *Journal of Structural Engineering, ASCE*, **115**(11), 2794-2809.
 16. Chang, G.A., and Mander, J.B. (1994). “Seismic Energy Based Fatigue Damage Analysis of Bridge Columns: Part I- Evaluation of Seismic Capacity”, Technical Report NCEER-94-0006. Buffalo (NY), State University of New York at Buffalo.
 17. Ramberg, W.A. and Osgood, W.R. (1943). “Description of Stress-Strain Curves by Three Parameters”, Technical Note No. 902, National Advisory Committee for Aeronautics.
 18. Martinez-Rueda, E. and Elnashai, A.S. (1997). “Confined Concrete Model under Cyclic Load”, *Material and Structures*, **30**, 139-147.
 19. Lokuge, W.P., Sanjayan, J.G., and Setunge, S. (2004). “Constitutive Model for Confined High Strength Concrete Subjected to Cyclic Loading”, *Journal of Materials in Civil Engineering, ASCE*, **16**(4), 297-305.
 20. Candappa, D.P., Sanjayan, J.G., and Setunge, S. (2001). “Complete Triaxial Stress-Strain Curves of High-Strength Concrete”, *Journal of Materials in Civil Engineering, ASCE*, **13**(3), 209-215.
 21. Attard, M.M. and Setunge, S. (1996). “Stress-Strain Relationship of Confined and Unconfined Concrete”, *ACI Materials Journal*, **93**(5), 432-442.
 22. Lavassani, H.H., Tasnimi A.A., and Soltani M. (2009). “A Complete Hysterical Constitutive Law for Reinforced Concrete under Earthquake Loadings”, *Journal of earthquake Engineering and Seismology (JSEE)*, **11**(1).
 23. Yankelevsky, D.Z. and Reinhardt, H.W. (1987a).

- Model for Cyclic Compressive Behavior of Concrete”, *Journal of Structural Engineering, ASCE*, **113**(2), 228-240.
24. Li, B., Park, R., and Tanaka, H. (2000). “Constitutive Behavior of High-Strength Concrete under Dynamic Loads”, *ACI Structural Journal*, **97**(4), 619-629.
25. Kappos, A.J. and Konstantinidis, D. (1999). “Statistical Analysis of Confined high Strength Concrete”, *Material and Structures*, **32**(224), 734-748.
26. Li, B., Park, R., and Tanaka, H. (1994). “Strength and Ductility of Reinforced Concrete Members and Frames Constructed using High Strength Concrete”, Research Report 94-5, University of Canterbury, New Zealand, 373p.
27. Li, B., Park, R., and Tanaka, H. (2001). “Stress-Strain Behavior of High-Strength Concrete Confined by Ultra-High- and Normal-Strength Transverse Reinforcements”, *ACI Structural Journal*, **98**(3), 395-406.
28. Sakai, J. and Kawashima, K. (2006). “Unloading and Reloading Stress-Strain Model for Confined Concrete”, *Journal of Structural Engineering, ASCE*, **132**(1), 112-22.
29. Nagashima, T., Sugano, S., Kimura, H., and Ichikawa, A. (1992). “Monotonic Axial Compression Test on Ultra-High-Strength Concrete Tied Columns”, *Proceedings of the 10th World Conference on Earthquake Engineering*, Balkema Rotterdam, The Netherlands, 2983-2988.
30. Cusson, D. and Paultre, P. (1994). “High-Strength Concrete Columns Confined by Rectangular Ties”, *Journal of Structural Engineering, ASCE*, **120**(3), 783-804.
31. Razvi, S. and Saatcioglu, M. (1996a). “Tests of High-Strength Concrete Columns under Concentric Loading”, Rep. No. OCEERC 96-03, Ottawa Carleton Earthquake Engineering Research Centre, Ottawa, ON, Canada, 147p.
32. Muguruma, H., Watanabe, F., Iwashimizu, T., and Mitsueda, R. (1983). “Ductility Improvement of High Strength Concrete by Lateral Confinement”, *Trans. Jpn. Concr. Inst.*, **5**, 403-410.

Notation

- b_c = center-to-center width of the perimeter tie
 C_i = center-to-center distance between laterally supported longitudinal bars
 d_c = center-to-center height of the perimeter tie
 d_s = diameter of the ties (circular hoop or spiral)
 E_c = tangent modulus of elasticity of concrete
 E_{sec} = secant modulus of elasticity
 E_t = modulus of elasticity of concrete acting in tension
 f'_c = specified concrete compressive strength
 f'_{cc} = confined concrete compressive strength
 f_{yh} = yield strength of the transverse reinforcement steel
 f_y = yield strength of the longitudinal reinforcement steel
 f'_t = tensile concrete strength
 s = spacing between the ties
 α = modified factor for calculating the effectiveness of confinement
 ε_c = axial concrete strain in general
 ε_{cc} = strain at maximum confined strength of concrete f'_{cc}
 ε_{co} = compressive strain at maximum in-place unconfined concrete strength f'_c
 ε_{pl} = plastic strain
 ε_{un} = unloading concrete strain
 ε_t = tensile concrete strain in general
 ε_{ro} = initial concrete stress on reloading branch
 $\varepsilon_{0.35f'_{cc}}$ = strain at which stress in confined concrete drops to $0.35f'_{cc}$
 $\varepsilon_{0.5f'_{cc}}$ = strain at which stress in confined concrete drops to $0.5f'_{cc}$
 ρ_h = volumetric ratio of transverse reinforcement
 ρ_g = volumetric ratio of longitudinal reinforcement
 σ_c = concrete stress in general
 σ_{new} = degraded concrete stress
 σ_{un} = reversal envelope stress
 σ_{ro} = initial concrete stress on reloading branch
 σ_t = tensile concrete stress in general